Research Paper

Efficacy of Single Acupoint and Compatible Acupoints on Oxidative Stress Amelioration in Diabetic Gastroparesis Rats

YUAN WANG, JIAZHEN CAO[1], YING WANG[2], DI WU[2], YANGMEI SHENG[2], XIN JIA[2], LIJUAN HA[2] AND XIAONA LIU[2]*

Department of Chinese Medicine, Second Affiliated Hospital of Heilongjiang University of Chinese Medicine, [1]Department of Nursing, [2]Acupuncture and Moxibustion Academy, Changchun University of Chinese Medicine, Changchun, Jilin Province 130117, China

The aim of this study was to observe the effect and mechanism of single point and compatibility acupoints on diabetic gastroparesis rats. The effect difference between single point and compatible points of diabetic gastroparesis rat's model rats was evaluated by hematoxylin and eosin, immunohistochemistry and Western blot. The expression of Cajal, neuronal nitric oxide synthase, nuclear factor erythroid 2-related factor 2 and heme oxygenase-1 proteins in gastric tissue and the expression of hypothalamic mesencephalic intestinal peptides neuronal nitric oxide synthase, ghrelin and somatostatin proteins were observed. Compared with the model group, the mediastinal and circumferential muscle cells of the gastric smooth muscle of CV12 and ST36 were relatively compact. The grooves of stomach were slightly changed, and the main cells, adenium cells and cervical mucous cells were arranged more neatly than those in model group. Macrophages decreased in gastric submucosa and mucosal muscle layer. The arrangement of muscle cells in the mediastinal muscle layer and the circumferential muscle layer of CV12+ST36 gastric smooth muscle was relatively dense, which was more obvious than that in single point CV12 and ST36. After acupuncture treatment, the expression of neuronal nitric oxide synthase in gastric and hypothalamic were all increased compared with model group. In the expression of interstitial cells of Cajal, CV12+ST36 was better than CV12 than ST36. And compared with model group, the expression of nuclear factor erythroid 2-related factor 2 and heme oxygenase-1 was increased, and CV12+ST36 group was higher than that of single point CV12 and ST36 ($p<0.01$). In terms of central regulation, the expression of somatostatin protein in hypothalamus was observed in the single point group CV12 (2955.43±206.24, $p<0.01$), the combined point group CV12+ST36 (2066.88±116.81, $p<0.01$) was increased compared with model group. The expression of ghrelin in hypothalamus decreased in CV12 (76.00±6.16, $p<0.01$), but increased in ST36 (288.00±31.12, $p<0.01$). And CV12+ST36 (234.00±19.95, $p<0.05$) was increased after acupuncture treatment. The compatibility of acupoints is an important part of acupuncture treatment. Acupuncture improved gastric smooth muscle, the number and structure of interstitial cells of Cajal, and mucosal protection, and the compatibility acupoints was better than the single point, which may be increased the nuclear factor erythroid 2-related factor 2 and heme oxygenase-1 expression to protect diabetic gastroparesis rat's from oxidative stress.

Key words: Diabetic gastroparesis, acupuncture, nuclear factor erythroid 2-related factor 2, heme oxygenase-1, oxidative stress, cajal, neuronal nitric oxide synthase

Diabetic Gastroparesis (DGP) is a common complication of diabetes characterized by gastric dysmotility. Symptoms associated with DGP include early satiety, vomiting, nausea, and abdominal distention[1]. It is estimated to affect approximately 300 out of every 100 000 individuals, with a 5 y cumulative incidence of 2.1 % in type 1 diabetes and 0.2 % in type 2 diabetes[2]. The predominant Western medical approach for DGP involves using erythromycin as the first-line drug; however, >40 % of patients are unable to tolerate it due to severe side effects[3]. Acupuncture has been recommended as an alternative treatment for gastroparesis in the ACG's

***Address for correspondence**
E-mail: 460398946@qq.com

Accepted 02 September 2024
Revised 06 May 2024
Received 21 April 2023
Indian J Pharm Sci 2024;86(5):1652-1662

clinical management guidelines, with increasing evidence supporting its effectiveness[4,5].

Oxidative stress plays a direct role in diabetes development and its related complications, with DGP exacerbating oxidative stress levels[6]. This leads to the downregulation of Heme Oxygenase-1 (HO-1), subsequently causing damage to Interstitial Cells of Cajal (ICC) and impairment in gastric emptying. Nuclear factor erythroid 2-related factor 2 (Nrf2) and HO-1 as a pivotal protein in mitigating oxidative damage across various tissues and organs. Extensive research indicates that is the crucial in safeguarding tissues and organs against oxidative stress-induced harm[7,8]. Based on the above research, we hypothesize that the improvement of ICC pacing function by electroacupuncture is related to the regulation of oxidative stress. Therefore, this study established a rat model of DGP to observe the regulation of Nrf2 and HO-1 expression in Cajal cells by electroacupuncture. We aim to elucidate the potential mechanism of electroacupuncture in treating DGP and the differences in efficacy between single acupoints and paired acupoints, laying the foundation for acupoint selection in DGP treatment.

MATERIALS AND METHODS

Experimental reagents and preparation:

A Streptozotocin (STZ) citrate buffer was prepared as follows; 2.10 g of citric acid was dissolved in 100 ml of distilled water, and 2.949 g of sodium citrate was dissolved in another 100 ml of distilled water. Subsequently, 50 ml of each solution was combined and pH adjusted to 4.5. The STZ (Sigma) powder was then dissolved in the freshly prepared citric acid buffer at pH 4.5 to create an STZ solution with a concentration of 0.1 mol/l.

Animals:

All animal-related procedures adhered to guidelines and regulations for the ethical care and use of animals in experimentation, and received approval from Changchun University of Traditional Chinese Medicine's Experimental Animal Ethics Committee (Approval No: 2022163). 100 Sprague-Dawley (SD) rats, with an average weight of (200±20) g, were procured from Liaoning Changsheng Biotechnology Co. The rats were accommodated in sanitized animal facilities maintained at 22°±3°, 50 %-60 % relative humidity, under a 12 h/12 h light-dark cycle with standard nutrition and *ad libitum* access to water.

DGP model:

Rats underwent a 1 w acclimatization period and were fed accordingly. Prior to experimentation, all rats tested negative for urine sugar using urine glucose test strips, and those with positive results were excluded. Following a 12 h fast, the rats received a single injection of 0.1 mol/l STZ citrate buffer into the left lower abdominal cavity at a dosage of 50 mg/kg body weight. Model induction was confirmed 72 h later when non-fasting blood glucose levels exceeded 16.7 mmol/l.

Experimental design:

In the subsequent phase, rats were randomly assigned to the following groups, normal group has no interventions; model group has DGP model induced without treatment; CV12 group with electroacupuncture at CV12; ST36 group with electroacupuncture at ST36 and CV12+ST36 group with simultaneous electroacupuncture at CV12 and ST36.

Acupuncture points were located according to the experimental acupuncture and moxibustion and the rat acupuncture point atlas. Electroacupuncture parameters included; continuous wave, 20 Hz, 3.0 mA, 15 min stimulation each session, once daily for 5 d per course of treatment. To prevent overstimulation or acupoint fatigue, there was a 1 d break between courses, totalling 3 w of treatment.

Measurement of blood glucose:

Blood samples were retrieved from the rats' tail veins, and blood glucose levels were measured using a one touch blood glucose meter and test strips.

Gastric emptying rate:

The rats underwent a 10 h fasting period prior to sampling, and each group received an oral gavage of Indian ink at 1 ml/100 g. Subsequently, after 30 min, the rats were euthanized *via* cervical dislocation. The abdominal cavity of each rat was meticulously opened, and the intestinal cavity was delicately lifted and straightened using forceps before being placed flat on the table. The gastrointestinal advancement index was then calculated by measuring the distance from the upper end to the pylorus and the lower end to the ileocecal region with a straightedge. The rate of the gastrointestinal advancement index was determined using the formula:

Gastrointestinal advancement rate=(distance from the front end of the ink to the pyloric sphincter (cm)/ distance from the pyloric sphincter to the end of the small intestine (cm))×100 %

Histopathological procedure:

Samples of gastric tissues from each group were collected and then stored in 10 % neutral formalin fixative overnight. Subsequently, standard paraffin-embedded sections (3 μm) were prepared and stained with Haematoxylin and Eosin (H&E) for histopathological analysis.

Perfusion sampling:

The rats were anesthetized with 2 % pentobarbital, adjusted based on their body weight. Following this, the rats were positioned with the abdomen facing upward, and the thorax was incised. A small opening was made in the apical part of the left ventricle using a scalpel. A 20-gauge needle was inserted into the ascending aorta, secured in place, and the descending aorta was clamped shut with a hemostatic forceps. Additionally, a small opening was created in the right auricle to instil 300 ml of saline. The rinsing process continued for approximately 12 min until colourless and clear fluid started to flow from the right atrium. Subsequently, 500 ml of a 4° fixative solution was injected for about 23 min to complete the perfusion. Rats that did not pass the perfusion test were excluded. The rat's heads were held in one hand while the skull was carefully removed with forceps in the other hand to fully expose the brain. The brain tissue was collected and fixed in 4 % paraformaldehyde for 12 h, followed by three washes with a Phosphate Buffered Saline (PBS) solution. Dehydration in 30 % sucrose was performed for 4 h-8 h, followed by three additional washes with PBS. The tissue was then treated overnight at 4° in 15 % sucrose. A customized cassette was prepared, the tissue block was placed flat inside, and a small cup with an appropriate amount of liquid nitrogen was prepared. The cassette was placed flat in the cup, ensuring the block touched the liquid nitrogen to induce rapid freezing. This step was carefully monitored for approximately 20 s until the tissue solidified into a block.

Immunohistochemical assessment:

The tissue samples were fixed in 10 % neutral formalin fixative overnight. Subsequently, routine paraffin-embedded sections underwent immunostaining. Initially, the sections were dewaxed in xylene for 15 min and then rehydrated with a diluted ethanol solution. Following this, the sections were incubated in Triton solution for 20 min and rinsed with PBS for 4 min. Antigen retrieval was performed by immersing the tissue sections in boiling repair solution (pH=6.0 citrate buffer) for 5 min. After cooling for 40 min, the sections were washed three times for 5 min each with PBS, incubated in a humid chamber with a drop of primary antibody overnight at 4°. The subsequent day, the sections were washed again with PBS thrice for 5 min each, incubated in a humid chamber with a universal secondary antibody at 37° for 40 min. Following another round of PBS washes, the sections were subjected to 3,3′-Diaminobenzidine (DAB) colour development solution in the humid chamber. The tissue coloration process was observed under a microscope and terminated at the appropriate level. To complete the process, haematoxylin restraining was carried out, the sections were cleared in xylene I and II for 5 min each, mounted with gum, and coverslips were applied and levelled carefully. Evaluation of the sections was conducted under an optical microscope, and quantitative image analysis using image analysis software (ImageJ, 1.48, National Institutes of Health (NIH), United States of America (USA)) was performed for immunohistochemical assessment.

Assessment of stomach levels:

The tissue pieces were cut as finely as possible with scissors, then ground with liquid nitrogen and protein lysis solution for 30 min. Subsequently, the solution was transferred to a centrifuge tube, and loading buffer was added before being heated at 95° for 10 min. The gel plate was secured onto the electrophoresis tank, and running buffer was poured between the plates. Marker (3-4 μl) and each sample were added sequentially, the box was covered, and the gel was run for 1 h at which point the film was run by current at 250 mA for 90 min. Afterward the film was removed, placed on a paper towel, and dried. Following staining, the membrane was immersed in water and washed, then cut along the outer sides of the upper and lower markers based on the molecular weight of the target index. The membrane was further washed with TBST for 5 min each, twice. Subsequently, the rinsed membrane was placed in a cassette and shaken for 1 h. A primary antibody (1:1000) was added and left to shake overnight at 4°. The following day, the primary antibody was removed at -20°, the membrane was washed with Tris-Buffered Saline with 0.1 % Tween® 20 detergent (TBST) thrice for 5 min each time, and then a secondary antibody was applied. The membrane underwent another round of washing with TBST for 10 min each, three times. Finally, excess TBST was removed, a luminescent solution was applied, and the membrane was exposed to chemiluminescence using a Tennant Western blot auto-exposure instrument. The film was developed and

fixed post-exposure. Statistical analysis was conducted using Statistical Package for the Social Sciences (SPSS) 18.0 software, and experimental data were presented as mean±Standard Error of the Mean (SEM). Normality testing was initially performed, followed by either a two-group t-test (Student's t-test) for parametric data or a nonparametric rank sum test for non-normally distributed data. A significance level of $p<0.05$ was set to denote statistical significance.

RESULTS AND DISCUSSION

As shown in Table 1, the gastric emptying rate in the model group significantly decreased ($p<0.01$), indicating successful modelling. Compared with the model group, the gastric emptying rate in the ST36 group significantly increased ($p<0.01$), while the gastric emptying rate in the CV12 group decreased ($p<0.05$), with better performance in the ST36 group than the CV12 group. This indicates that electroacupuncture at ST36 can promote gastric movement, while electroacupuncture at CV12 has the opposite effect, inhibiting gastric motility.

The H&E staining results of the gastric tissues indicated a reduction in the cytoplasm of the smooth muscle in both the middle longitudinal and circular layers in the model group (fig. 1). Additionally, the cytoplasm of smooth muscle cells in the mucosal layer displayed light staining, transparency, and visible vacuole-like changes. Uneven grooves were observed in the gastric notch, with misaligned glands, decreased principal cell count, irregular arrangement, and enlarged cell gaps. Furthermore, the wall cell cytoplasm showed reduced staining, presence of vacuole-like changes, and congestion in the mucosa and submucosa. Vascular dilation was evident, along with an increased number of macrophages in the submucosa compared to the normal group. Compensatory thickening of the mucosal muscle layer was noted, albeit with non-uniform thickness. In the CV12 and ST36 group, there was a relatively dense arrangement of myocytes in the middle longitudinal and circular smooth muscle layers of the gastric muscle. The grooves in the gastric notch showed minor changes, with well-aligned main cells, glandular cells, and cervical mucus cells compared to the model group. A reduction in submucosal macrophages was observed, and there was slight improvement in the mucosal muscle layer compared to the model group, resulting in a relative reduction in macrophages. Particularly in the group receiving acupuncture at the ST36+CV12 points, the arrangement of myocytes in the smooth muscle of the gastric muscle showed a notably dense pattern. The grooves of the gastric notch displayed slight modifications, and the main cells, glandular cells, and cervical mucus cells were more neatly arranged compared to the model group. Overall, there were slight enhancements in the submucosal and mucosal muscle layers of the stomach, along with a relative reduction in macrophages.

The Immunohistochemical analysis of gastric ICC revealed a considerable presence of brownish-yellow granules in the normal rat gastric tissue (fig. 2), particularly surrounding the intermuscular plexus between the cricoid muscle and longitudinal muscle layer, forming a sheath-like structure around ganglion cells. In contrast, the model group exhibited a minimal amount of lightly stained brownish-yellow granules amidst the gastric muscles. Conversely, the CV12 and ST36 single-acupuncture point groups displayed abundant darkly stained brownish-yellow granules among the gastric muscles. Moreover, the group with matching acupuncture points outperformed the single acupuncture point groups. Significant disparities in c-kit protein expression were identified between the control and model groups ($p<0.001$), as well as between the acupuncture and model groups ($p<0.05$). Furthermore, a highly significant contrast was observed between the matching point group and the single CV12 acupuncture group ($p<0.001$), as well as the ST36 group ($p<0.05$). Notably, within the treatment groups, both the matching point and CV12 groups demonstrated superior outcomes compared to the ST36 group.

TABLE 1: COMPARISON OF GASTROINTESTINAL PROPULSION RATE IN EACH GROUP AFTER ACUPUNCTURE

Group	Gastrointestinal propulsion rate (%)
Normal	80.5±7.49**
Model	46.80±18.25
ST36	65.77±12.36**
CV12	37.78±9.46*
ST36+CV12	52.93±8.1*

Note: Data are presented as the mean±standard error, *$p<0.05$ and **$p<0.01$ compared with model group

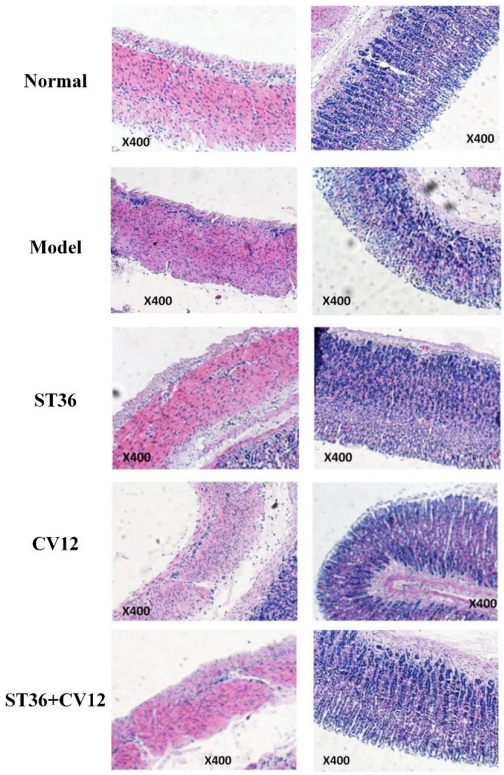

Fig. 1: H&E staining results of gastric muscle layer in rats (400X)

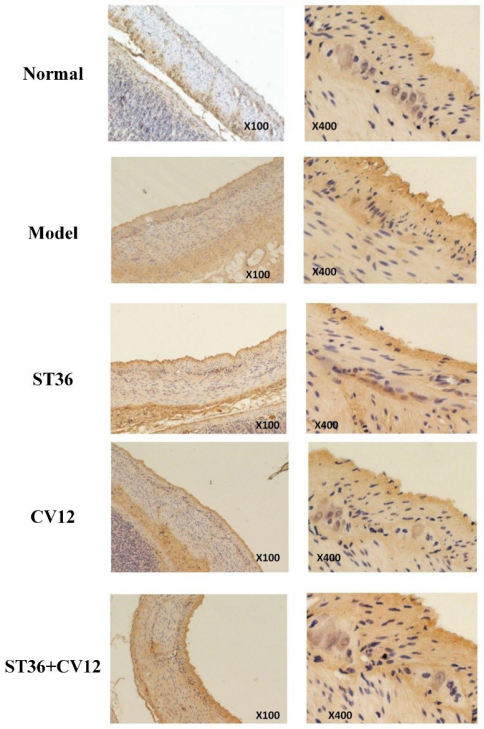

Fig. 2: Immunohistochemistry of Cajal in in gastric tissue (100X and 400X)

Neuronal Nitric Oxide Synthase (nNOS) was expressed in the gastric intermuscular plexus and hypothalamus across all rat groups (fig. 3). Immunohistochemical analysis revealed abundant brownish-yellow granules in the gastric tissue of normal rats, predominantly around the intermuscular plexus between the cricoid muscle and the longitudinal muscle layer, showing consistent and intense staining. Conversely, the model group exhibited a sparse presence of lightly stained brownish-yellow granules, significantly fewer than the control group. Rats in the CV12 and ST36 single-acupuncture point groups displayed a moderate number

of lightly stained brownish-yellow granules amidst the gastric muscles, indicating an increase compared to the model group. In the matched-acupuncture point group, a substantial number of darkly stained brownish-yellow granules were observed between the stomach muscles, surpassing those in the model group. Moreover, the ST36 group exhibited a higher granule count than both the CV12 group and ST36+CV12 group.

The Nrf2 protein immunohistochemistry results revealed minimal brownish-yellow granules between the annulus and longitudinal muscle layers in the normal rat group (fig. 4). The cytoplasm was predominantly visible, with very few nuclei and light staining. In contrast, the model rat group exhibited an abundance of brownish-yellow granules between the annulus and longitudinal muscle layers, with visible nuclei and cytoplasm displaying dark staining. The CV12 and ST36 rat groups showed a sparse presence of brownish-yellow granules between the annulus and longitudinal muscle layers, where the nuclei and cytoplasm were noticeable, and the staining appeared slightly darker. Additionally, the matching point group demonstrated a moderate number of brownish-yellow granules between the circular and longitudinal muscle layers in the gastric tissues, with dark staining in the nucleus.

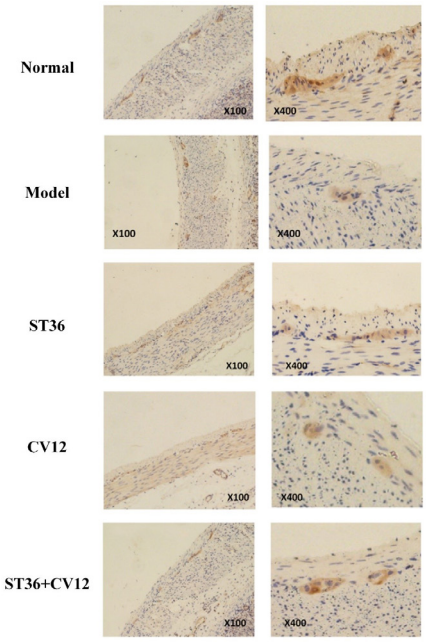

Fig. 3: Immunohistochemistry of hypothalamic nNOS protein

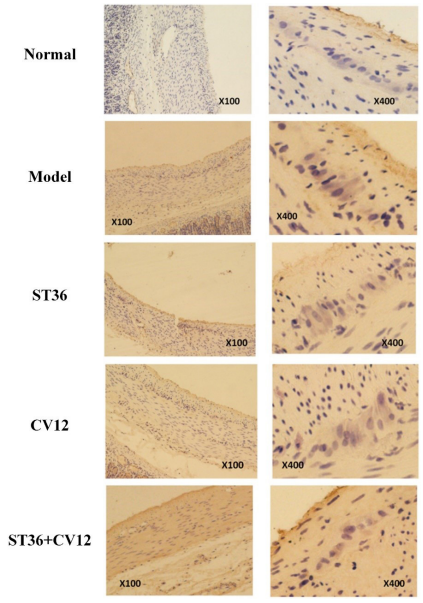

Fig. 4: Immunohistochemistry of gastric Nrf2 protein (100X and 400X)

The immunohistochemically analysis of the protein HO-1 revealed minimal brownish-yellow particles with light staining in the annulus and longitudinal muscle layer of the normal rat group (fig. 5). Conversely, the model rat group exhibited a substantial presence of brownish-yellow particles with dark staining in the same area. The CV12 and ST36 groups displayed a modest amount of brownish-yellow particles with slightly darker staining, while the matching point group showed a moderate number of brownish-yellow particles with light staining. The particles appeared lightly stained in all cases.

Both Nrf2 and HO-1 proteins were detected at Cajal sites. Nrf2 exhibited positive expression in the Cajal cytoplasm and nucleus, appearing in shades of tan or light brown. In contrast, HO-1 was found in the cytoplasm in a tan hue, with limited to no expression in the nucleus.

The Nrf2 and HO-1 expression levels were significantly higher in all treatment groups compared to the normal group ($p<0.001$). Moreover, the expression was notably greater in the matched acupuncture point group than in the single acupuncture groups CV12 and ST36 ($p<0.001$), with no significant difference observed between the CV12 and ST36 groups ($p>0.05$). Thus, acupuncture potentially exerts a gastro protective effect by increased the Nrf2 and HO-1 protein in DGP rats. This aids in alleviating oxidative stress damage in gastric Cajal mesenchymal cells.

Ghrelin protein expression in the hypothalamus varied among groups of rats (fig. 6). Protein expression levels were lower in the CV12 group (76.00±6.16, $p<0.01$) compared to the model group (168.00±14.97). Conversely, the ST36 group (288.00±31.12, $p<0.01$) exhibited higher expression than the model group. In the matching point group, protein expression was elevated (234.00±19.95, $p<0.05$). Furthermore, a significant difference was observed between the single-acupuncture point ST36 group and the matching point group ($p<0.05$).

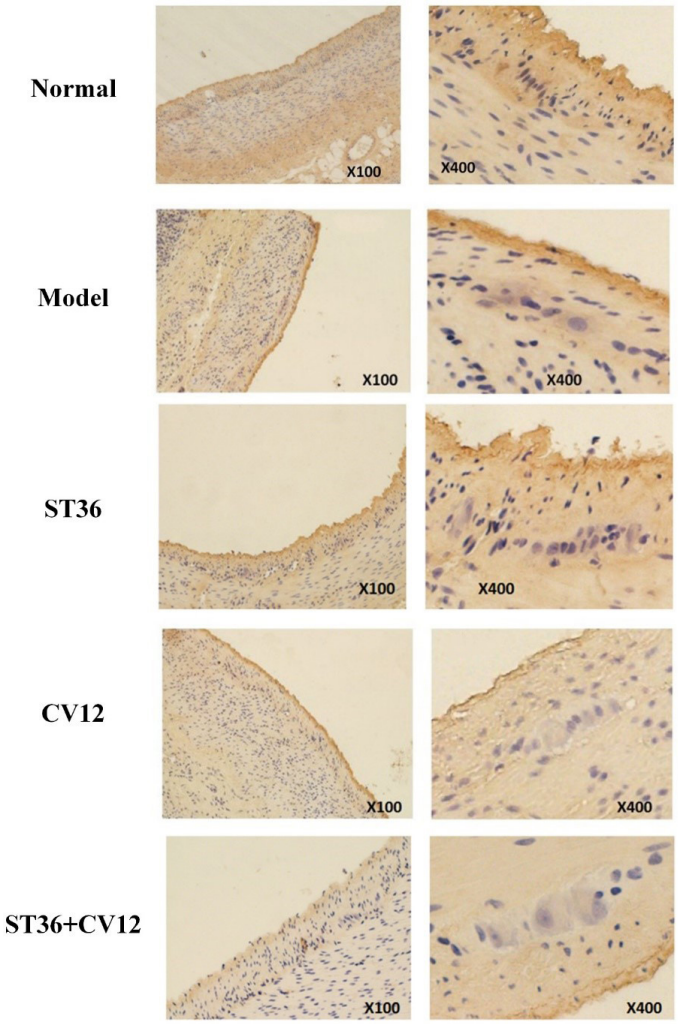

Fig. 5: Immunohistochemistry of gastric HO-1 protein (100X and 400X)

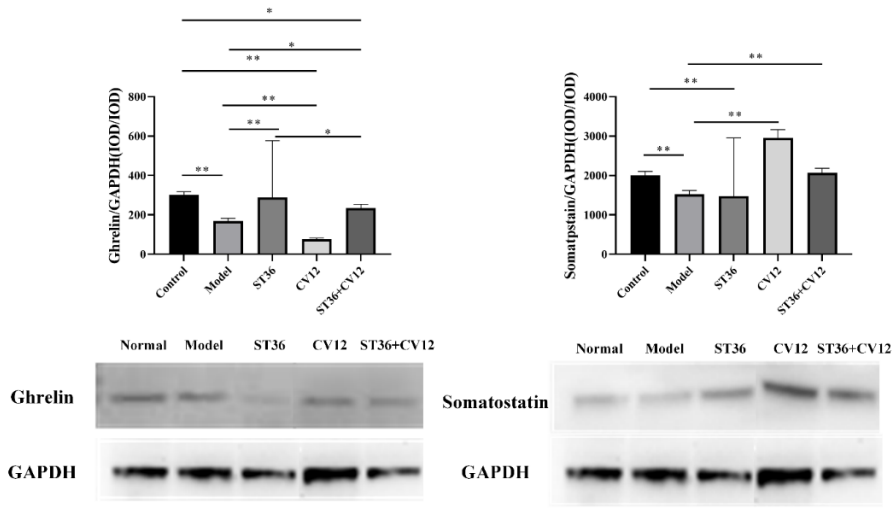

Fig. 6: The expression of ghrelin and somatostatin in hypothalamus

Single-Stranded (SS) proteins are expressed in the hypothalamus. Rats in the DGP model exhibited varying alterations (fig. 6). Specifically in the single-acupuncture point group, the CV12 group (2955.43±206.24, $p<0.01$) demonstrated higher expression levels compared to the model group (1522.25±99.64), with no significant differences observed in the ST36 groups. In the collocation group, the CV12+ST36 group (2066.88±116.81, $p<0.01$) displayed elevated expression levels when compared to the model group.

In our study, we observed that the distal acupoint ST36 enhanced gastric motility, while the proximal acupoint CV12 inhibited gastric motility, aligning with previous research[9]. Acupuncture facilitated the restoration of gastric smooth muscle and ICCs, with the combined use of CV12+ST36 showing superior efficacy compared to CV12 or ST36 alone. Furthermore, acupuncture shielded DGP rats from oxidative stress damage by increased the Nrf2 and HO-1 protein, with CV12+ST36 displaying enhanced effectiveness over CV12 or ST36 individually. Moreover, regarding the regulation of ghrelin and SS in the central hypothalamus, the comprehensive regulatory impact of acupuncture at the paired acupoints exceeded that of a single point.

ICCs are specialized cells located between smooth muscle cells and enteric neurons in the digestive tract, serving as gastrointestinal slow-wave pacemakers responsible for generating and propagating slow waves[10]. ICCs play a crucial role in maintaining normal gastrointestinal motility. Structural damage or ICC reduction can impair gastrointestinal pacing, leading to smooth muscle motor contraction weakness, diminished peristalsis, and the manifestation of gastrointestinal motility disorders impacting gastric function[11]. Experimental models in diabetic mice have exhibited a significant reduction in ICCs within the gastric body and antrum[12]. Research indicates that over 50 % of individuals with diabetes develop gastric motility disorders, affecting their health and quality of life [13]. Restoring ICC function by increasing their number and repairing damaged structures may be pivotal in the treatment of DPG. Electroacupuncture has been shown to upregulate ICC expression, decreased the expression of LC3 and P62, ease the suppression of autophagy to improve gastric motility[14]. Combining acupuncture with electrical stimulation at CV12, ST25, and ST36 has been demonstrated to boost ICC numbers and repair their ultrastructural damage[15]. Our study compared the effects of single-point CV12 and ST36 *vs*. the combined acupoints CV12+ST36 on ICC content and cell repair, revealing the superior efficacy of the combined acupoints over the single-point stimulation.

DGP is a prevalent clinical complication of diabetes, characterized by chronic hyperglycemia leading to gastric motility issues such as early satiety, vomiting, and nausea[16]. Research has demonstrated that oxidative stress can be triggered by elevated blood sugar and high levels of Free Fatty Acids (FFA)[17]. Activation of oxidative stress signalling pathways may lead to impaired insulin secretion, Insulin Resistance (IR), and diabetic vasculopathy[18,19]. Hence, oxidative stress plays a significant role in the development of type 2 diabetes and its late complications. Antioxidant therapy is considered a potent strategy in preventing and managing diabetes and its associated complications. Numerous studies have validated that Nrf2 triggers increased expression of HO-1 under oxidative stress

conditions, effectively shielding the body from harm[20-22]. Reducing oxidative stress concurrently safeguards the normal levels and nutritional status of essential nutrient factors crucial for the differentiation of ICCs precursor cells. This protection ensures the maintenance of a healthy ICC source and the equilibrium of ICC population[23]. Prior research has demonstrated that DGP can elevate the oxidative stress response, leading to a reduction in HO-1 levels[6]. The subsequent decrease in HO-1 expression results in damage to ICCs and delays in gastric emptying[24]. The overexpression of HO-1 leads to the accumulation of excess Fe^{2+} and Carbon dioxide (CO_2), potentially elevating cellular oxidative stress levels, causing mitochondrial damage, and compromising cell integrity in specific conditions[25]. As a result, Nrf2 plays a pivotal role in safeguarding cells against diverse stress-induced injuries[26]. Our research revealed that HO-1 and Nrf2 were expressed in the ICCs in DGP rats but were rarely detected in the control group. In the experimental group, staining at the CV12+ST36 acupoint site was lighter compared to individual CV12 and ST36 points. The Nrf2 expression in both cytoplasm and nucleus was higher in the combined acupoint group than in the single-point group. HO-1 was identified in the cytoplasm with shades of brown and yellow, demonstrating higher positive expression in the combined acupoint group than in the single-point group. This study validates the hypothesis of a strong correlation between ICCs and oxidative stress response. Acupuncture exhibited protective effects against oxidative stress-induced damage in gastric ICCs of DGP rats, potentially through the increased Nrf2 and HO-1 protein expression. The combined stimulation of CV12 and ST36 acupoints showed superior protective effects compared to individual stimulation at CV12 or ST36.

The investigation of acupuncture point compatibility represents a fundamental scientific inquiry in the advancement of acupuncture and moxibustion. It also embodies the historical responsibility of modern acupuncture and moxibustion practitioners. Acupoint combinations are implemented based on the principles of syndrome differentiation and treatment, where two or more acupoints with similar functions are harmonized to enhance their synergistic effects[27]. The traditional theory of combining acupoints can significantly enhance the therapeutic outcomes compared to using a single acupoint. It not only utilizes the individual functions of each acupoint but also leverages synergistic interactions between them, allowing for mutual reinforcement and ultimately amplifying the clinical efficacy[28,29]. Through extensive literature review, our team conceptualized the notion of same gong points, proposing that acupoints used in combination should possess similar therapeutic effects[30]. In recent years, global experimental studies have revealed that acupuncture regulation can influence the mechanism of gastric motility regulation, leading to a notable improvement in symptoms associated with gastric dysfunction like nausea, vomiting, and abdominal distension post-acupuncture treatment[31]. However, despite numerous studies on acupuncture for DGP, there is a lack of comparative reports on the efficacy of single-point *vs*. combination acupoint treatments for DGP management. Hence, this study aimed to investigate the distinctions between individual acupoints and compatible acupoint combinations in addressing diabetic gastric dyskinesia while following the TCM meridian theory. Li *et al*.[32] conducted research on rats using acupuncture along with electrical stimulation, discovering that stimulating CV12 inhibited gastric motility, while ST36 promoted. Li *et al*. concluded that acupuncture's impact on gastrointestinal motility involves benign regulation through neurologic, endocrine, and immune mechanisms, facilitating bidirectional modulation that could restore gastrointestinal function[33]. Research on the activation of the vagoadrenal axis through Prokineticin receptor 2 (Prokr2)-Cre labelled sensory neurons revealed that low-intensity electroacupuncture stimulation at ST36 triggered the vagoadrenal anti-inflammatory pathway, contrasting with the inefficacy of abdominal ST25[34]. The study provides the neuroanatomical foundation for the selection and specific functions of acupoints. Focusing on DGP, this research examines the impact of individual acupoints (CV12, ST36) and combination acupoints (CV12+ST36) on regulating gastric motility by assessing the expression levels of hypothalamic ghrelin (a gastric motility and emptying promoter) and somatostatin (a gastric emptying inhibitor). Initially, single acupoints were found to excel in certain individual measurements compared to combination acupoints, yet a holistic evaluation across multiple parameters favoured the compatibility acupoints. Nonetheless, the depth of investigation into the central mechanisms is acknowledged as needing enhancement, while exploring the synergistic effects of various acupoint combinations holds critical implications for elucidating acupoint specificity in future studies.

Acknowledgments:

This research was supported by National Natural Science Foundation of China (No: 81804172) based

diseases and spleen and stomach meridian characterization.

Authors' contributions:

Lijuan Ha and Xiaona Liu have contributed equally to this work.

Conflict of interests:

The authors declared no conflict of interests.

REFERENCES

1. El Halabi M, Parkman HP. 2023 update on the clinical management of gastroparesis. Expert Rev Gastroenterol Hepatol 2023;17(5):431-41.
2. Dilmaghani S, Zheng T, Camilleri M. Epidemiology and healthcare utilization in patients with gastroparesis: A systematic review. Clin Gastroenterol Hepatol 2023;21(9):2239-51.
3. Yamada M, Hongo M, Okuno Y, Nishimura N, Ueno M, Kawakami H, *et al*. Effect of AS-4370 on gastric motility in patients with diabetic autonomic neuropathy. J Smooth Muscle Res 1992;28(4):153-8.
4. Yu B, Sun M, Wang Z, Zhu B, Xue J, Yang W, *et al*. Effects of stimulating local and distal acupoints on diabetic gastroparesis: A new insight in revealing acupuncture therapeutics. Am J Chin Med 2021;49(5):1151-64.
5. Kim KH, Lee MS, Choi TY, Kim TH. Acupuncture for symptomatic gastroparesis. Cochrane Database Syst Rev 2018;12(12).
6. Kashyap PC, Choi KM, Dutta N, Linden DR, Szurszewski JH, Gibbons SJ, *et al*. Carbon monoxide reverses diabetic gastroparesis in NOD mice. Am J Physiol Gastrointestinal Liver Physiol 2010;298(6):G1013-9.
7. Sampath C, Sprouse JC, Freeman ML, Gangula PR. Activation of Nrf2 attenuates delayed gastric emptying in obesity induced diabetic (T2DM) female mice. Free Radic Biol Med 2019;135:132-43.
8. Alruhaimi RS. Protective effect of arbutin against cyclophosphamide-induced oxidative stress, inflammation, and hepatotoxicity *via* Nrf2/HO-1 pathway in rats. Environ Sci Pollut Res Int 2023;30(26):68101-10.
9. Lin X, Levanon D, Chen JD. Impaired postprandial gastric slow waves in patients with functional dyspepsia. Dig Dis Sci 1998;43:1678-84.
10. Takaki M. Gut pacemaker cells: The Interstitial Cells of Cajal (ICC). J Smooth Muscle Res 2003;39(5):137-61.
11. Sanders KM, Kito Y, Hwang SJ, Ward SM. Regulation of gastrointestinal smooth muscle function by interstitial cells. Physiology 2016;31(5):316-26.
12. Ordög T, Takayama I, Cheung WK, Ward SM, Sanders KM. Remodeling of networks of interstitial cells of Cajal in a murine model of diabetic gastroparesis. Diabetes 2000;49(10):1731-9.
13. Bharucha AE, Kudva YC, Prichard DO. Diabetic gastroparesis. Endocr Rev 2019;40(5):1318-52.
14. Wei X, Lin Y, Zhao D, Xiao X, Chen Q, Chen S, *et al*. Electroacupuncture relieves suppression of autophagy in interstitial cells of Cajal of diabetic gastroparesis rats. Can J Gastroenterol Hepatol 2020;2020(1):7920715.
15. Lin G, Zhang J, Li L, Zou Z, Chen C, Xue L, *et al*. Effect of electroacupuncture on gastric interstitial cells of Cajal in a rat model of diabetic gastroparesis. Exp Ther Med 2016;11(6):2489-94.
16. Marathe CS, Rayner CK, Wu T, Jones KL, Horowitz M. Gastrointestinal disorders in diabetes. Diabetes 2024.
17. Jiang Y, Xu L, Zhu X, Zhu X, Xu X, Li J. Hyperglycemic stress induces oxidative damage of enteric glial cells by triggering redoxosomes/p66SHC activation. Redox Rep 2024;29(1):2324234.
18. Zeng S, Wang Y, Ai L, Huang L, Liu Z, He C, *et al*. Chronic intermittent hypoxia-induced oxidative stress activates TRB3 and phosphorylated JNK to mediate insulin resistance and cell apoptosis in the pancreas. Clin Exp Pharmacol Physiol 2024;51(3):e13843.
19. Rodiño-Janeiro BK, González-Peteiro M, Ucieda-Somoza R, González-Juanatey JR, Álvarez E. Glycated albumin, a precursor of advanced glycation end-products, up-regulates NADPH oxidase and enhances oxidative stress in human endothelial cells: Molecular correlate of diabetic vasculopathy. Diabetes Metabol Res Rev 2010;26(7):550-8.
20. Nguyen T, Yang CS, Pickett CB. The pathways and molecular mechanisms regulating Nrf2 activation in response to chemical stress. Free Radic Biol Med 2004;37(4):433-41.
21. McCubrey JA, LaHair MM, Franklin RA. Reactive oxygen species-induced activation of the MAP kinase signaling pathways. Antioxid Redox Signal 2006;8(9-10):1775-89.
22. Tagawa A, Kaneko T, Shinohara T, Ueda A, Sato T, Ishigatsubo YJ. Heme oxygenase-1 inhibits cigarette smoke-induced increase in the tracheal mucosal permeability in guinea pigs *in vivo*. Inflamm Res 2005;54:229-34.
23. Izbeki F, Asuzu DT, Lorincz A, Bardsley MR, Popko LN, Choi KM, *et al*. Loss of Kitlow progenitors, reduced stem cell factor and high oxidative stress underlie gastric dysfunction in progeric mice. J Physiol 2010;588(16):3101-17.
24. Choi KM, Gibbons SJ, Nguyen TV, Stoltz GJ, Lurken MS, Ordog T, *et al*. Heme oxygenase-1 protects interstitial cells of Cajal from oxidative stress and reverses diabetic gastroparesis. Gastroenterology 2008;135(6):2055-64.
25. Wang L, Zhou Y, Lin H, Hou K. Protective effects of Relaxin 2 (RLXH2) against hypoxia-induced oxidative damage and cell death *via* activation of the Nrf2/HO-1 signalling pathway in gastric cancer cells. Cell J (Yakhteh) 2023;25(9):625.
26. Kobayashi A, Ohta T, Yamamoto M. Unique function of the Nrf2-Keap1 pathway in the inducible expression of antioxidant and detoxifying enzymes. Methods Enzymol 2004;378:273-86.
27. Jun ZH, Xia LI, Zheng H, Kun YE, Xin WA, Xuefei WA, *et al*. Effects of acupuncture on functional gastrointestinal disorders: Special effects, coeffects, synergistic effects in terms of single or compatible acupoints. J Tradit Chin Med 2023;43(2):397.
28. Liu L, Wu Y, Zheng J, Lai X, Zeng D, Li H, *et al*. Cerebral activation effects of acupuncture using Zusanli (ST36) and Yanglingquan (GB34) points based on regional homogeneity indices: A resting-state fMRI study. J X-Ray Sci Technol 2016;24(2):297-308.
29. Xuefen W, Ping L, Li L, Xiaoli C, Yue Z. A clinical randomized controlled trial of acupuncture treatment of gastroparesis using different acupoints. Pain Res Manag 2020;2020(1):8751958.
30. Jiang HL, Xu XH, Zhao JY, Wang FC. Acupoint compatibility effect: Increasing effect value and expanding effect domain.

Zhongguo Zhen Jiu 2023;43(11):1275-8.
31. Guo Y, Wei W, Chen JD. Effects and mechanisms of acupuncture and electroacupuncture for functional dyspepsia: A systematic review. World J Gastroenterol 2020;26(19):2440.
32. Li YQ, Zhu B, Rong PJ, Ben H, Li YH. Effective regularity in modulation on gastric motility induced by different acupoint stimulation. World J Gastroenterol 2006;12(47):7642.
33. Li X, Liu S, Liu H, Zhu JJ. Acupuncture for gastrointestinal diseases. Anat Record 2023;306(12):2997-3005.
34. Liu S, Wang Z, Su Y, Qi L, Yang W, Fu M, *et al*. A neuroanatomical basis for electroacupuncture to drive the vagal-adrenal axis. Nature 2021;598(7882):641-5.